JOURNAL OF OPTOELECTRONICS AND ADVANCED MATERIALS Vol. 10, No. 1, January 2008, p. 174 - 184

A study of field dependent steady-state photocarrier grating measurements for microcrystalline semiconductors using different theoretical methods

R. I. BADRAN
Physics Department, King Abdulaziz University, Jeddah, Saudi Arabia
(On leave from The Hashemite University, Zarqa, Jordan)

The study of field dependent steady-state photocarrier grating (SSPG) measurements has been performed on microcrystalline samples prepared by hot-wire chemical vapor deposition (HWCVD) technique. The field-dependent experimental data at room temperature are analyzed using different approaches based on the small-signal photocurrent to extract more information on the electronic properties (like drift mobility for electrons and holes, small signal mobility life time product, average drift length for holes and electrons,… etc.). The quality of the fits has been tested by χ^2 indicator and the best choice of the transport parameters has been extracted due to each adopted approach. The trapped charge density can be correlated to minority-carrier mobility-lifetime product or diffusion length which is, in turn, may be related to sub-gap absorption.

(Received October 3, 2007; accepted January 10, 2008)

Keyword: (Amorphous semiconductors; glasses), (Electronic transport phenomena in thin films), (Charge carriers: generation, recombination, lifetime, trapping, mean free paths), (Photoconduction and photovoltaic effects).
Section: Semiconductor Physics

1. Introduction

In recent years amorphous and microcrystalline semiconductors have been investigated worldwide as essential materials for solar cells, photosensors, large area flat displays, and light emitting diodes (LED). This is because of their abundance, non-expensive cost, high absorption coefficient in the visible spectra range and low processing temperature. Also easy doping and alloying of these materials are important reasons for the wide usage of them [1]. The most important candidates of amorphous and microcrystalline semiconductors are hydrogenated silicon and germanium films, prepared by either plasma enhanced chemical vapor deposition (PECVD) or hot wire chemical vapor deposition (HWCVD) techniques. Therefore, intensive studies on electronic and optical properties of these materials become very necessary. Several techniques have been developed such as time of flight, surface photovoltage (SPV) [2], and steady state photocarrier grating (SSPG) techniques for this purpose. Among the most important techniques are those which have been developed for measuring the effective diffusion length for amorphous semiconducting materials. Usually these techniques are based on the collection of minority carriers at some known distance from the region where they are created, as is the case, for example, for the well-known Haynes-Schockley technique [3]. Another technique that involves the collection of minority carriers but requires the existence of a rectifying junction is the surface photovoltage (SPV) technique [3]. The steady-state photocarrier grating (SSPG) technique differs from previous types of techniques in that it does not involve collection of minority carriers, but it is based on the concept of creating a gradient in carriers concentration, which controls the sample conductivity. This conductivity becomes a highly sensitive function of diffusion of the charge carriers.

The SSPG became a highly competitive technique in the experimental study and analysis of the electrical properties of amorphous semiconducting materials because it is simple setup and easy to perform by experimentalists [3-5]. This technique also provided the most accurate way in the determination of the true bulk diffusion length [3]. The knowledge of the ambipolar diffusion length L_{amb} is of a great importance for the performance of several semiconducting devices like, bipolar transistors and photovoltaic cells. In particular, its value in hydrogenated amorphous silicon (a-Si:H) and related materials is known to be a good indicator of the suitability of a film for solar cell application.

In steady state photocarrier grating (SSPG) technique, the sample is illuminated by two coherent light beams, I_1 and I_2, of different intensities that interfere and create gratings $\Delta G(x)$ superimposed on a uniform generation G_0 [3-5]. In the standard application of SSPG, the photocurrent response under the presence of spatially modulated photogeneration in amorphous semiconductors is measured at low electric fields. The characteristic transport length is determined by diffusion and its value in comparison to the grating period determines the extent to which diffusion smears out the photocarrier grating. If the grating period is much greater than the carrier diffusion length, well-defined photocarrier concentration grating is created in an amorphous semiconductor sample. On the

other hand, if the grating is comparable to or smaller than the diffusion length, an almost uniform carrier concentration occurs inspite of the nonuniform generation [3-8]. The detection of photocarrier grating amplitude is a good probe for determining the diffusion length [3-5]. The measurement of small signal conductivity in SSPG depends on the grating period Λ which, in turn, varies as the angle of incidence of the two laser beams changes. The photocurrent density measured either when the two beams interfere to generate gratings which caused a non-uniform spatial distribution of carrier densities that leads to an ac photocurrent called J_{coh} or when the beams do not interfere where the generated carrier density and then the photocurrent, J_{incoh} , are due to a pure bias illumination. The measured ratio ($\beta = \frac{J_{coh}}{J_{incoh}}$) and its relation to the grating period give the estimated observed value of ambipolar diffusion length, L_{amb} [3, 4]. Therefore the photoconductivity of a small spatial modulation (or grating) of photocarrier concentration amplitude depends on $L_{amb.}$ The excitation of photocarriers from trap states creates space charge effects in the sample. The generation of the space charges is controlled by both mobile and trapped carriers. The tendency of generating space charges becomes high when the most mobile carriers (electrons) move away faster than the less mobile carriers (holes). The change in the external field from low values to high values results consequently in a change from diffusion-dominated to drift-dominated transport process.

Another important feature in using SSPG technique over other techniques is clearly appeared in the convenient theoretical treatment of SSPG problem [3-8] that may provide us with information about the transport parameters of the investigated thin film semiconductors such as mobility lifetime product $(\mu\tau)$ for charge carriers …etc, in addition to the ambipolar diffusion length.

An outstanding progress in understanding the transport and recombination of photocarriers of a semiconductor using SSPG experiment was achieved when this experiment was carried out at high electric fields. The SSPG transport equations were solved, via different approaches [3, 6-8], on the basis of a small-signal grating of optical excitation superimposed on a much stronger uniform background generation of electron-hole pairs, by considering both lifetime and relaxation time regimes. In one approach [6], the development of SSPG analysis was based on the free carriers concentration and their extended states mobility-lifetime products. An analytical expression for the coefficient β which is a function of both grating period and electric field, was obtained using an analytical approach. This analytical expression is validated by conducting numerical calculations. Here, the carrier recombination process was handled phenomenolgically without adopting a model that accounts for the microscopic mechanisms. In another approach [7], the analytical treatment of steady-state transport equations in the small signal case based on the perturbation expansion theory, to the first order, was conducted. General expression for the change in photocurrent was derived for the case of a small SSPG finite electric field when space charge effects are taken into account [7]. It was assumed that the photocurrent is considerably larger than the dark current and under such circumstances the average mobility of photocarriers does not differ from that of dark carriers. The average mobility over all mobile and trapped carriers was considered constant for each type of carriers. The solution of the SSPG transport equations in the small-signal approximation was extended thereafter to the second order in perturbation, in a third approach [8]. The latter approach has the advantage of avoiding previous assumptions of restriction on local charge neutrality and in considering the drift mobility and effective diffusion coefficient for electron and holes as concentration dependent. Therefore the correction of the SSPG theory in the relaxation-time regime was implemented and the importance of space charge effects was revealed in this regime. A global expression for the coefficient β was found and showed to contain two components relevant to drift and diffusion currents. An extended technique to measure accurately the diffusion length by removing the inherent defects in the original SSPG theory, was demonstrated by a successful application to hydrogenated amorphous silicon [8].

This paper concentrates on the investigation of the field dependence of the coefficient β and the transport parameters by studying the experimental data for microcrystalline silicon thin film samples, according to Abel *et. al*., Li and Hattori *et. al*. approaches [8]. The samples were prepared by HWCVD technique in ultra-high vacuum system [9]. The application of these approaches on such experimental data may enable us to extract important information on the electronic properties (like drift mobility for electrons and holes small signal mobility-lifetime product of charge carriers and recombination lifetime) and to estimate the trapped carrier density. The correlation among the transport parameters may also allow us to estimate other important physical quantities like the drift and diffusion lengths for electrons and holes. The diffusion length which was determined from fitting the experimental data in the low-field diffusion regime was employed to fit the experimental data for the wide range of electric fields [10]. We found that this assumption could be adopted within the illumination level of the conducted SSPG experiment for the microcrystalline samples under investigation. We have also used the expression for the density of states (DOS), from the exploitation of SSPG technique, which was derived for amorphous semiconductors [11-14] in order to roughly estimate DOS for the microcrystalline samples. The values of density of states from this expression are compared to those extracted from the three adopted approaches.

2. Theoretical background

Several SSPG theories developed on the basis of small-signal approaches relate the magnitude of the

measured photocurrent with the ambipolar diffusion length. The formulas obtained from these theories were used in the analysis of SSPG experimental data. The ambipolar diffusion length can be extracted from fitting low electric field data [3-5]. However, further study of high electric field data in addition to low electric field data allow the possible monitoring of diffusion- to drift-dominated transport phenomena [6-8].

If, N_0 and P_0, are uniform background electrons and holes densities in the absence of coherence between I_1 and I_2, then $\Delta N(x)$ and $\Delta P(x)$, are grating densities of photoelectrons and photoholes, respectively due to the presence of coherency. However, $N\ (P)$ represents the total density of electrons (holes) rather than the mobile carriers alone. For non-crystalline semiconductors $N\ (P)$ is the sum of free and trapped electrons (holes) [3, 7].

In the absence of a strong electric field and under the assumption of local charge neutrality, i.e. electrons and holes diffuse together with approximately equal diffusion coefficients, so that the concentration of excess electrons and holes is equal, $\Delta N = \Delta P$. Under these conditions the space charge completely smears out, the diffusion of charge carriers is ambipolar rather than bipolar and is represented by ambipolar diffusion length, L_{amp} and a common carrier recombination lifetime τ (or the small-signal photocurrent response time from the steady state, under uniform excitation of G_0), is given by $\frac{1}{\tau} = \left.\frac{\partial R}{\partial N}\right|_{G_0} = \left.\frac{\partial R}{\partial P}\right|_{G_0}$, where R is the recombination rate. In the presence of strong electric field the space-charge effects become prominent and the process is rather bipolar.

The solution to the transport equations was found on the basis of the perturbation expansion theory, in the first order, and on the small signal approach [7]. An expression for the coefficient β, which is dependent on both the grating period and electric field, was obtained [11], as well; namely:

$$\beta = 1 - \frac{\left(\frac{g_1\tau}{N_0}\right)^2\left(\frac{a(a+\ell^2)}{2}\right)\left(1+\frac{1}{\gamma(I_2/I_1)}\right)}{\left(\left(a+\frac{(b+1)^2}{4b}\ell^2\right)(1+\ell^2)+d^2\right)^2+\frac{(b-1)^2}{4b}d^2} \qquad (1)$$

The transport parameters, $l\left(=\frac{2\pi L_{amb}}{\Lambda}\right)$, $a\left(=\frac{\tau}{\tau_{diel}}\right)$, $b\left(=\frac{\mu_n}{\mu_p}\right)$, and $d\left(=\frac{2\pi\sqrt{\mu_n\mu_p\tau}E_0}{\Lambda}\right)$ are shown to have special physical meanings [7]. Here, E_o, μ_n and μ_p are the external electric field, the free carrier mobilities of electrons and holes, respectively. The dielectric relaxation time τ_{diel} is defined in Ref. 7. The parameter γ corresponds to the exponent in the power-law light intensity dependence of photoconductivity. Here g_1 is the amplitude of the small signal modulated grating rate, $\Delta G(x) = g_1\cos(kx)$. If $g_1 << G_0$ then the linearization condition for solving the transport equation is satisfied. This condition implies that the thermal energy divided by grating period Λ must be greater than the maximum potential energy associated with the oscillating internal electric field amplitude.

In another approach [8], the transport equations were solved, with assumptions made to avoid the pitfalls of the original SSPG analysis [3-5, 7]. The first assumption was to include the effect of the space-charge at higher electric fields in addition to the case of local charge neutrality at low fields. Another assumption was made considering the drift mobility and effective diffusion constant as concentration dependent parameter. The SSPG theory was also extended by including second order term in perturbation. A more accurate form of the coefficient β was derived [8]:

$$\beta = 1 - 2\gamma\gamma_0^2\Gamma\,. \qquad (2)$$

The parameter γ is given, here, by, $\gamma = (\mu_n' + \mu_p')\tau'/(\mu_n + \mu_p)\tau$ and γ_o is a grating quality factor that explains the reason beyond a possible faint visibility of the gratings which may be resulted from light scattering, mechanical vibrations, non-ideal polarization,.. etc. A common small-signal lifetime is defined as $\tau' = \frac{\tau_n'\tau_p'}{\tau_n' + \tau_p'}$, where τ_n', τ_p' and τ are as in Ref. 8. The drift mobility for electrons and holes $\mu_n(N)$, and $\mu_p(P)$ were defined in terms of free electron (hole) mobility, free electron (hole) concentration and total electron (hole) concentration $N\ (P)$ [8]. $\mu_n'(N)$ and $\mu_n'(P)$ which are called small-signal mobility for electrons and holes, respectively, are first order terms in the drift mobility and were defined in terms of the unperturbed parameters [8]. We will consider, here, a simplified version of the SSPG parameter, Γ by neglecting some minor terms in the original expression [8], namely; $\Gamma = \frac{n_k p_k \sin(\Phi)}{KL_{diel}}$, where $K = \frac{2\pi}{\Lambda}$, n_k and p_k are the normalized grating amplitudes of electron and hole concentrations. The grating amplitudes, in their final forms, were obtained [12] and introduced in the original expression for coefficient β. The dielectric relaxation length, L_{diel} and the phase shift, Φ between electron and hole concentration gratings were defined in

Ref. 8. However, the dimensionless transport parameters were defined as $b \equiv \frac{\mu_n}{\mu_p}, a \equiv \frac{\tau'}{\tau_{diel}}, \delta = \frac{\tau'}{\tau'_n}$, and $\eta = \frac{\tau'}{\tau'_p}$, where $\delta + \eta = 1$ [8]. Here, another dimensionless constant $b' = \left(\mu'_n / \mu'_p = L_{en} / L_{ep} = L^2_{dn} / L^2_{dp}\right)$ can be introduced as well. The dielectric relaxation time τ_{diel} is same as before [7, 8].

A general theoretical approach [6] was established to study the influence of the external electric field, in addition to the grating period, on the change of the photocurrent response. It was suggested that the change in photocurrent response probes the charge from diffusion-to-drift-dominant transport while the electric field is varying over a wide range of values, in the SSPG technique. The derivation of a small signal formula which considers both non-ambipolar and bipolar, in addition to the effect of external field, was achieved. The main advantage of the derived formula for $\beta(E, \Lambda)$ is in its dependence on both the grating period and external electric field. This derivation required, in advance, numerical solution to both continuity equations for electrons and holes in addition to Poisson's equation in order to establish the boundary conditions necessary for analytical approach. In particular, an analytic formula for the coefficient β, which depends on both the grating period Λ and the external field E, contains different characteristic drift and diffusion transport lengths. Such lengths are responsible for identifying the drift and diffusion dominant transport mechanism.

In case of dominance of one charge carrier type (like electron, for example) β has the following form [6, 10].

$$\beta = 1 - 2\gamma \frac{1 + \left(2\pi L^{(5)}_{diff} / \Lambda\right)^2}{\left(1 + \left(2\pi L^{(1)}_{diff} / \Lambda\right)^2 + \left(2\pi L^{(2)}_{diff} / \Lambda\right)^4 + \left(2\pi L^{(3)}_{drift} / \Lambda\right)^2\right)^2 + \left(2\pi L^{(4)}_{drift} / \Lambda\right)^2}. \quad (3)$$

where, $L^{(1)}_{diff}$, $L^{(2)}_{diff}$, $L^{(3)}_{drift}$, $L^{(4)}_{drift}$ and $L^{(5)}_{diff}$. are as defined in Ref. 6.

Two adjustable parameters γ and τ^{eff}_{rel} are used to fit the experimental data. The parameter $\tau^{eff}_{rel} = \frac{n_0 \tau_{diel}}{N_0}$ is an effective relaxation time, which includes the time of the trapped photocarrier after thermal re-emission and their contribution to the conventional dielectric relaxation time under illumination, $\tau_{diel} \approx \frac{\varepsilon_r \varepsilon_0}{e n_0 \mu_n}$. The parameter n_0 is the free carrier density and N_0 is the total carrier density (free plus localized). μ_n and μ_p are, as defined before, the free carrier mobilities of electrons and holes, respectively. The mobility lifetime product of the holes $\left(\mu_p \tau_p\right)$ can be determined from the fit to the low-field experimental data and inserted as input data in the high field fit. This approach has been employed to fit experimental data of field dependence of β at different grating periods for different microcrystalline samples at different temperatures [10].

3. Experimental

The microcrystalline silicon thin film samples used here were prepared by HWCVD technique under ultra-high-vacuum system [9].

A source of red laser diode is used in a standard experimental set-up for steady-state photocarrier grating measurements like that used elsewhere [10, 15, 16]. The sample is fixed within an evacuated cryostat where the optical components, which are mounted on a movable plate, have to be moved instead of the sample in order to change the grating period. The red laser diode is fixed on the table such that the laser beam travels almost the same distance between the laser source and the sample at the full range of grating periods. The background uniform generation rate values for the samples I, II and III of thicknesses 0.39, 1.0 and 0.61μm are G_o = 6.37 × 10^{20}, 3.65 × 10^{20} and 4.9 × 10^{20} $cm^{-3}s^{-1}$, respectively. It is obvious, from Table 1, that the highest value of the product $\left(\mu\tau\right)_n$ is for sample II with the largest σ_{dark} while the lowest $\left(\mu\tau\right)_n$ value is for sample I with lowest dark conductivity (here, the dark conductivity of sample I could not be detected because it was lower than the limit of the measurable equipment). This behavior is similar to that shown by other groups for microcrystalline silicon samples [16]. The experimental data of field-dependent β for the three samples are shown in Figs. 1 and 2.

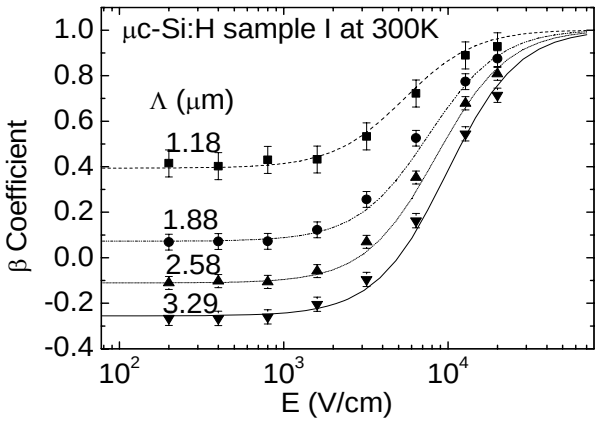

Fig. 1. The coefficient β versus electric field for μc-Si:H sample I at room temperature. Both theoretical results (lines) and experimental data (symbols) are taken at different grating periods. The theoretical results are found using Abel et. al. approach [6].

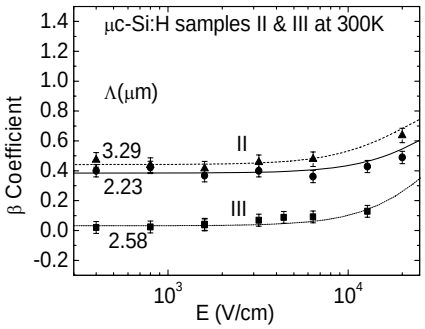

Fig. 2. The same as in figure 1, but for μc -Si:H samples II and III at 300 K.

4. Results and discussion

In a similar analysis to that conducted [11] elsewhere the low field fit for different silicon samples has been done, and the obtained values of the dark conductivity, photoconductivity, the ambipolar diffusion length L_{amb}, φ, the majority and minority carriers lifetime product are summarized in Table 1.

Table 1. List of parameters used to fit the experimental data of β coefficient versus grating period, Λ, and extracted from the SSPG experiment for three microcrystalline silicon samples at room temperature.

μc -Si:H Sample	φ	$L_{amb}(nm)$	$(\mu\tau)_p \times 10^{-9}$ (cm^2V^{-1})	$(\mu\tau)_n \times 10^{-7}$ (cm^2V^{-1})	$\sigma_d \times 10^{-6}$ $(S.cm^{-1})$	$\sigma_{ph} \times 10^{-5}$ $(S.cm^{-1})$
I	0.70	147	4.18	0.126	0.0	0.13
II	0.34	86.0	1.45	3.37	15.86	1.97
III	0.48	54.4	0.61	3.25	4.72	2.56

4.1 Results due to application of Abel *et al.* approach

In order to fit the field dependence experimental data of β, using equation 3 [6], the value of $(\mu\tau)_p$ extracted from the low field fit and $(\mu\tau)_n$ taken from the experimental data (shown in Table 1) are employed as input data, in a FORTRAN computer program. Thus the adjustable parameters used to fit the experimental data are, $\mu_n\tau_{rel}^{eff}$ and γ. Fig. 1 shows the variation of the electric field dependence of β for the μc -Si:H sample I at room temperatures and grating periods. Also the fittings to experimental data of μc -Si:H samples II and III at 300 K are shown in Fig. 2. The best fits are obtained using the χ^2 indicator. The list of adjustable parameters and the χ^2 values are presented in Table 2.

Table 2. The list of parameters employed, using Abel et al. approach [6], to fit the experimental data of electric field dependence of β for different microcrystalline silicon samples at different grating periods and at room temperature. The least χ^2 values are also quoted.

μc -Si:H Sample	$\Lambda(nm)$	$\mu_n\tau_{rel}^{eff} \times 10^{-8}$ (cm^2V^{-1})	γ	χ^2
I	3290	0.3	0.77	1.771
	2580	0.25	0.75	0.575
	1880	0.29	0.84	0.669
	1180	0.16	0.9	0.144
II	3290	0.25	0.6	0.159
	2230	0.17	0.62	0.383
	1180	0.11	0.64	-
III	2580	0.14	0.5	0.230

4.2 Results due application of Li approach

A FORTRAN program is developed where a, μ_n, μ_p and g_1/N_0 are used as adjustable parameters. This allow easily finding the values of τ, b and N_0, respectively. The fitting of all experimental data of field-dependent β started with values of $\frac{\mu_n}{\mu_p}$ (or b) and $\frac{\tau}{\tau_{diel}}$ (or a) near to or greater than unity in order to avoid breaking the linearization condition for a finite excitation grating [7]. Each of the used adjustable parameters is changed within a range of reasonable values based on the physical grounds. Each choice of parameters gives us the calculated result of β which is compared to that of corresponding experimental data. However, the program allows us to iterate all possible values of combination of parameters and calculate the χ^2 as an indicator to get the best fit to experiment. The best choice of parameters is taken when the value of χ^2 is minimum. However, the use of the values of L_{amb} extracted from low field fit and inserted as input data in the field dependence fit is found reasonable at the chosen values of *a*. The ratio I_2/I_1 is given a value of 0.06 and $\tau_{diel} = \frac{\varepsilon_\circ \varepsilon_r}{\sigma_{ph}}$ is used for all the fits. The value of external applied field E_0 is taken equal to $\left(\frac{2}{\sqrt{b}L_{amb}}\frac{k_B T}{e}\right)$. The variation of the electric field dependence of β for the μc-Si:H samples I and (II, III) at 300 K and different grating periods are shown in Figs. 3 and 4, respectively. The theoretical results (lines) are obtained using the minimum χ^2 values. Table 3 lists all adjustable parameters and χ^2 values.

Table 3. List of parameters employed to fit the experimental data of electric field dependence coefficient β for different microcrystalline silicon samples at room temperature and different grating periods, using Li approach [7]. The minimum χ^2 values obtained from the fittings are also listed.

μc-Si:H Sample	$\Lambda(nm)$	$a = \frac{\tau}{\tau_{diel}}$	$\mu_n \times 10^{-2}$ ($cm^2V^{-1}s^{-1}$)	$\mu_p \times 10^{-2}$ ($cm^2V^{-1}s^{-1}$)	g_1/N_0 $\times 10^5 (s^{-1})$	χ^2
I	3290	1.37	0.80	0.110	2.44	4.525
	2580	1.50	0.80	0.110	2.44	4.387
	1880	1.57	0.80	0.110	2.44	1.707
	1180	1.62	0.80	0.110	3.20	0.309
II	3290	0.50	0.90	0.395	1.30	0.351
	2230	0.77	0.80	0.396	1.87	0.747
	1180	0.99	0.80	0.397	1.90	-
III	2580	0.70	0.90	0.428	2.80	0.305

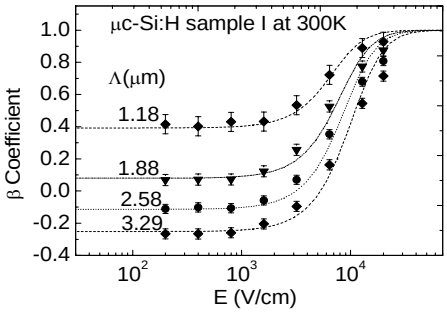

Fig. 3. The field dependence experimental data (symbols) of the coefficient β for μc-Si:H sample I at different grating periods and at room temperature. The theoretical results (lines) are obtained using Li approach [7].

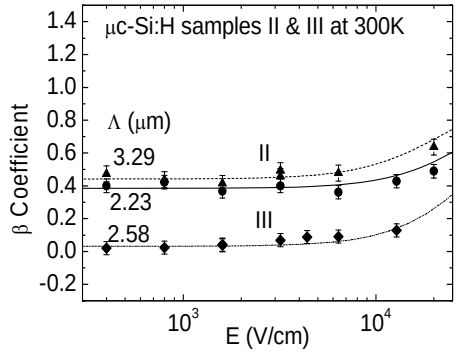

Fig. 4. The same as in figure 3, but for μc-Si:H samples II and III at 300 K.

The other criterion for satisfying the linearization condition has also been tested via finding the product of (g_1/N_0) and τ. It is worth noting, as an example, for μc-Si:H sample I at $\Lambda = 3290nm$ that a value of $g_1\tau \approx 2.27\times10^{14}\,cm^{-3}$ can be compared to the value of charge density $N_0 = 8.77\times10^{14}\,cm^{-3}$ found from equation 58 of Ref. 7. Unfortunately $g_1\tau$ is not much less than N_0 as predicted [7]. Also $g_1 = 2.14\times10^{20}\,cm^{-3}s^{-1}$ is obviously not very much less than $G_0 = 6.376\times10^{20}\,cm^{-3}s^{-1}$. Analogous results for the other samples show similar trend.

An increase in the value of μ_p causes a decrease in the value of β at high electric fields. While an increase in the value of μ_n leads to an increase in the value of β at high electric fields. However, these two parameters exhibit opposite effects at low values of electric field, as well. This gives values of $b = 7.6\pm0.3$ and $b = 2.1\pm0.18$ at different grating constants for samples I and II, respectively. Such values represent the tendency towards generating space charges. The other parameter has values $a = 1.51\pm0.15$ and $a = 0.7\pm0.17$ for samples I and II, respectively. These values measure the ability of the semiconducting sample to neutralize photocarrier-related space charge. Here both parameters a and b compete with each other within comparable uncertainties. Although a is not greater than b for all samples at $300K$, the value of a is still greater than $\frac{b\ell^2}{4}$ and satisfies the condition for maintaining charge neutrality even at the value of external field $E_0 \approx \frac{2}{\sqrt{b}L_{amb}}\frac{k_BT}{e}$. It is interesting to mention here, that the values of parameters a and b obtained from the fit indicate that the weak field condition $d^2 << \ell^2$ and, the strong field condition $d^2 >> \ell^2$ are not satisfied while other conditions are satisfied. This means that the chosen values are effective and transparent in the transition region between diffusion-dominated and drift-dominated processes.

4.3 Results due to application of Hattori *et al*. approach

A computer code is developed and used to test Hattori *et al.,* approach on a set of experimental data. Reasonable fits are obtained to all experimental data using five adjustable parameters, namely, $\mu_n, \mu_p, \mu_n', \mu_p'$ and $a(=\tau'/\tau_{diel})$. The search for the precise values of these parameters is based on minimizing the errors between the experimental data and calculations using χ^2 as indicator. The best fits to experimental data are obtained when values of χ^2 is minimum. The fits to the experimental data of the coefficient β versus applied electric field at different grating periods, Λ, when the SSPG experiment is conducted at room temperature are presented for μc-Si:H sample I in Fig. 5. The value of $\gamma_0 \approx 1$, the values of γ and $\tau_{diel} = \frac{\varepsilon_\circ\varepsilon_r}{\sigma_{ph}}$ previously used in Li approach, are also employed here. Similar values for a as that obtained from Li fittings are also found, here, for all samples. The fitting parameters μ_n and μ_p are found invariant for each sample, as listed in Table 4. The increase in μ_p raises the values of β in low field region ($E < 1000\,V/cm$) and lowers the values of β in the high field region. However, the electron drift mobility, μ_n exhibits opposite effect to that of μ_p on β.

Table 4. The set of parameters employed to fit the experimental data of electric field dependence of β for different microcrystalline silicon samples at different grating periods and at room temperature, using Hattori et. al., is listed. Here $\delta = 1$, and $\eta = 0$ are chosen [8, 12].

μc-Si:H Sample	$\Lambda(nm)$	$a = \frac{\tau'}{\tau_{diel}}$	$\mu_n \times10^{-2}$ ($cm^2V^{-1}s^{-1}$)	$\mu_p \times10^{-2}$ ($cm^2V^{-1}s^{-1}$)	$\mu_n' \times10^{-3}$ ($cm^2V^{-1}s^{-1}$)	$\mu_p' \times10^{-3}$ ($cm^2V^{-1}s^{-1}$)	χ^2
I	3290	1.37	1.0	0.10	1.7	0.65	2.17
	2580	1.5	1.0	0.10	2.0	0.65	1.97
	1880	1.57	1.0	0.10	2.2	0.65	0.48
	1180	1.62	1.0	0.10	2.5	0.65	0.20
II	3290	0.50	1.3	0.57	1.9	1.49	0.17
	2230	0.77	1.3	0.57	2.3	1.26	0.50
	1180	0.92	1.3	0.57	2.4	1.26	-
III	2580	0.7	1.3	0.56	2.0	1.26	0.24

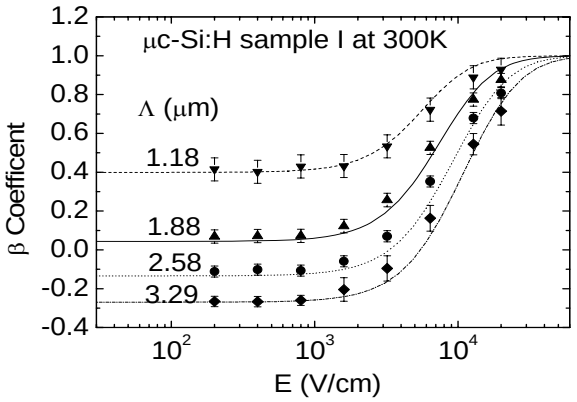

Fig. 5. The field dependence experimental data (symbols) of the coefficient β for μc-Si:H sample I at different grating periods and at room temperature. The theoretical results (lines) are obtained using Hattori et. al. approach [8].

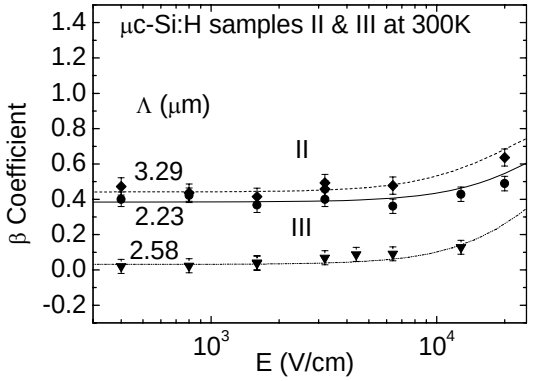

Fig. 6. The same as in Fig. 5, but for μc-Si:H samples II and III at 300 K.

The small-signal electron drift mobility μ_n' is found more sensitive than the hole drift mobility μ_p' in fitting the experimental data. This is reflected in the tolerance in the value of μ_n' of $\pm 0.4 \times 10^{-3}$ $cm^2V^{-1}s^{-1}$ for sample I and that of $\pm 0.2 \times 10^{-3}$ $cm^2V^{-1}s^{-1}$ for sample II. This can also be compared to negligible tolerance for sample III. However, the value of μ_p' is almost fixed for each sample but a tolerance of $\pm 0.45 \times 10^{-3}$ $cm^2V^{-1}s^{-1}$ is found among the three samples.

A reasonable fit could not be reached unless δ is close to unity at the given generation rates of $G_0 = 6.376 \times 10^{20}\, cm^{-3}s^{-1}$, 3.65×10^{20} and 4.9×10^{20} $cm^{-3}s^{-1}$, for μc-Si:H samples I, II and III, respectively. This assumption means that a larger value of hole lifetime τ_p' than that of the electron lifetime τ_n' is discernible.

A crude approximation can be made in determining the diffusion lengths $L_{dn,p}$ for electrons and holes using a simplified expression for the ambipolar diffusion length $L_{amb} = \left[\left(\mu_n L_{dp}^2 + \mu_p L_{dn}^2\right)/\left(\mu_n + \mu_p\right)\right]^{1/2}$ [8]. Here the value of ambipolar diffusion length obtained from the fit to experimental data at the low field can be used together with the transport parameters b and b' extracted from the electric field dependence of β, to estimate the values of L_{dn} and L_{dp}. The values of L_{dn} and L_{dp} which have been calculated using the obtained values of L_{amb}, from Table 1, together with the values of μ_n, μ_p, μ_n' and μ_p' from Table 4, are listed in Table 5 for the three samples.

Table 5. The calculated values of drift and diffusion lengths, $L_{en,p}$ and $L_{dn,p}$, for electrons and holes and average drift length of electrons and holes, $\langle L_{drift} \rangle$, are listed for the three samples.

μc-Si:H Sample	$\Lambda(nm)$	$L_{dn}(\mu m)$	$L_{dp}(\mu m)$	$L_{en}(\mu m)$	$L_{ep}(\mu m)$	$\langle L_{drift} \rangle (\mu m$	$(\mu_n' + \mu_p')\tau'$ $\times 10^{-9}$ (cm^2V^{-1})
I	3290	0.076	0.152	0.898	0.346	0.557	2.5
II	3290	0.093	0.826	0.013	0.010	0.011	0.05
III	2580	0.063	0.050	0.034	0.022	0.027	0.09

Further exploitation of the electric field dependence of β may allow estimations to the values of L_{en} and L_{ep}. This can be achieved if the assumption is made, that $E_0 \approx \frac{2\pi k_B T}{e\Lambda}$, in the transition region between the diffusion-dominated and drift-dominated transport regions. The obtained values for L_{en} and L_{ep} are listed in Table 5 for the three samples. Also knowing the formula for the average drift length of electrons and holes, $\langle L_{drift} \rangle = \left(\mu_n \mu_p\right)^{1/2} \tau E_0$ [7], enable us to find approximate values, for the three samples, when

$E_0 \approx \frac{2\pi k_B T}{e\Lambda}$ and the values of μ_n', μ_p' and τ' replace μ_n, μ_p and τ, respectively. The list of these values is also found in Table 5. Here the sample with lowest dark conductivity exhibits the largest value of $\langle L_{drift} \rangle$ while that with the highest dark conductivity has the lowest value.

The value of small-signal response lifetime τ' is very much consistent due to the application of both approaches of Li and Hattori *et. al*. The estimation of τ' allow us to estimate the mobility-lifetime product, namely, $(\mu_n' + \mu_p')\tau'$ for the three samples when the values of μ_n' and μ_p' from Table 4, are utilized. The results are listed in Table 5. It is worth comparing these values to values of similar product obtained due to the application of Li approach, $(\mu_n + \mu_p)\tau = 9.73\times10^{-9}$, 0.13×10^{-9} and 0.36×10^{-9} cm^2V^{-1} for samples I, II and III, respectively.

In all of the fits, for the three approaches, the deviation of theoretical results from experimental data is taken within an average of almost 10% of all experimental data at which the value of χ^2 is minimum. It is found that the least χ^2 values occurred in the Hattori *et al.* approach. The largest χ^2 values due to Li approach together with the poor quality of fits, for all of the samples, as compared to those of other values and fits, respectively, due to Hattori *et al.* and Abel *et. al.* approaches may reflect the weakness of the Li approach.

Our estimation to hole mobility values at room temperature disagree by two orders of magnitude with those measured by the transient photocurrent technique [17] and three order of magnitude by those found by the field-effect hole mobility measurement [18], but they agree with those measured by TOF experiment [19]. Moreover, the values of electron mobility differ by almost one order of magnitude to that measured by TOF experiment [19]. Our results also show that $\mu_n' \neq \mu_n$ which is an indication that both types of mobilities are dependent on concentration.

The utilization of our simplified expression of β in equation 21 of Ref. 8 is validated, as an example for μc-Si:H sample I at $\Lambda = 3290nm$, by obtaining the values of 0.15 and 0.325 for $\frac{\tau'}{\tau_n''}$ and $\frac{\mu_p''}{\mu_n'}$ when the values of μ_n, μ_p, μ_n' and μ_p' from Table 4, are used and $T = 300K$ and $T_V = 600K$ are considered.

4.4 Estimation of charge carriers density from different approaches

Due to Abel *et al*. approach, the trapped carrier density N_t can be obtained from the relation between the total carrier density N_0 [free plus localized] and $\mu_n \tau_{rel}^{eff}$, as $\mu_n \tau_{rel}^{eff} \approx (\varepsilon_r \varepsilon_0 / eN_0)$, by assuming that $(N_0 \approx N_t)$ i.e. the trapped carrier density is much higher than the free carrier density. The estimated values of N_t are listed in Table 6 for all samples.

By adopting the formula for the carriers charge density $N_0 \approx N_{ph} \approx \tau G_0 / \gamma$ due to Li approach [7], the calculated value of N_0 for sample I from Table 6 seems to have same value as that calculated using the same approximate formula but using τ' obtained from fit due to Hattori *et al.* approach instead of τ. However such formula may be appropriate for a photoconductive insulator, which has the very low dark conductivity [7]. These N_0 values can be compared to the corresponding values of N_0 obtained from Abel *et. al*. approach. However, the density of charge carriers, N_0, has also been determined using Schmidt-Longeaud formula [13, 14]. It is assumed that the photoconductivity replaces the factor σ_0 available in their formula of DOS for the sample under study. The value of N_0 is obtained from such formula is found in Table 6. The disagreement in the values of N_0 among applying Abel *et. al*. approach and the other approaches may be attributed to several approximations accompanied these latter approaches. The calculated values of N_0, using Schmidt-Longeaud formula are within the same order of magnitude to that obtained from capacitance measurements for pm-Si:H samples [20]. These values are also in agreement with other values reported in the literature [16] for microcrystalline samples although the used photon flux (1×10^{17} cm^{-2} s^{-1}) in our samples is different from that used in Ref. 11. Moreover the calculated values of N_0, due to Abel *et. al.* approach, are in agreement with those obtained by Reynolds *et. al.* [21]. The disagreement in the values of N_0 can be attributed to different factors. Firstly, the determination of SSPG-DOS, using Schmidt-Longeaud formula, may be not very precise for the microcrystalline silicon samples under study. This is because SSPG- DOS formula, which was derived for intrinsic amorphous silicon using several assumptions, might not be accurately applicable to the microcrystalline silicon samples under study and such formula may require further modification. In particular, the choice of the maximum value of Λ_{lim} =3.29 μm for our case may not lead to a good reproduction of the DOS. This value is far beyond the chosen value in the standard a-Si:H considered in Ref. 14. It must be noted that Schmidt-Longeaud formula was tested [14] by using standard values for the hydrogenated amorphous silicon parameters of μ_n and σ_o, which are different from those of the samples under study. In addition, the obtained values of DOS from this formula should be multiplied by μ_n/C_n, as suggested

by authors, when compared to the experimental data [14]. It must be also noted that the formula used to estimate N_0, due to Li and Hattroi *el. al.* approaches is "crudely" approximate, in the sense that only τ (or τ') varies with carrier density. Finally, the values obtained, here, for DOS can be ascribed, at most, to the density of deep defects in our samples. These values can also be compared to those of others [19, 20]. The values of N_0 in Table 6 together with the value of $(\mu\tau)_p$ in Table 1 may be considered as evidence for pronounced correlation between the trapped charge density and the minority carrier mobility-lifetime product, especially for samples II and III. The increase in sub-gap absorption is consistent with the much larger trapped charge density revealed in the field-dependent SSPG experiments.

Table 6. The comparison of estimated trapped charge density values for different μc-Si:H samples at room temperature, obtained from application of Li, Abel et. al., Hattori et. al. and Schmidt-Longeaud approaches [7, 6, 8, 13, 14].

μc-Si: H Sample	$\Lambda(nm)$	$N_0 \times 10^{14}$ $(cm^{-3}eV^{-1})$ (Li)	$N_0 \times 10^{14}$ $(cm^{-3}eV^{-1})$ (Abel)	$N_0 \times 10^{14}$ $(cm^{-3}eV^{-1})$ (Hattori)	$N_0 \times 10^{14}$ $(cm^{-3}eV^{-1})$ (Schmidt)
I	3290	342.5	851.5	342.5	7.75
II	3290	3.22	984.3	3.2	0.83
III	2580	10.6	1968.6	10.6	1.43

5. Conclusion

It is worth noting that the investigation of the hydrogenated microcrystalline semiconductor thin films, grown by hot-wire chemical vapor deposition technique using both the measurements and the SSPG theory gives us important information on the photoelectronic properties of this type of samples. The use of SSPG theory comprises three different approaches based on the small-signal photocurrent and involves the electric-field dependence in such technique. The experimental data obtained from SSPG technique that cover a wide range of applied electric field values, probe the whole transition region between the diffusion and drift-dominated transport. The ambipolar diffusion length is determined from fitting the experimental data in the low-field diffusion regime, and then employed in the fit of the experimental data for the whole range of electric fields. The transport parameters which have common physical grounds in the three approaches are correlated and used in an elegant way to fit the different available experimental data. The comparison of transport parameters among these approaches facilities the task of fitting experimental data and open “the door” for a self-contained analysis. This analysis also enables us to estimate several important parameters such as small-signal life time and small-signal mobility of both types of carriers. Moreover, the drift and diffusion lengths for holes and electrons can also be estimated. The exploitation of the electric-field dependence in the three approaches is correlating the photoelectronic properties, which are demonstrated by the transport parameters, to the trapped charge density which is usually not easily accessible. This may also justify the enhanced relationship between the minority carrier mobility-lifetime product and trapped charge density and then the sub-gap absorption in the sample under study.

Our theoretical investigation exposes the deficiencies in the original theory of low-field SSPG technique arising from the wrong application of the perturbation expansion theory in considering the first order term only and using mobility as concentration independent parameters. It also demonstrates the weakness in the assumption of local charge neutrality and ambipolarity restriction. The extracted transport parameters are found sensitive in the transition region that links the lifetime regime where the ambipolar transport takes place, with the relaxation time where the space-charge effects and bipolar transport become significant. We reckon that the analyses of experimental data of electric field dependence, due to the approaches of Abel *et al*., and Hattori *et al*., are more recommended than that of Li approach. Moreover, a well-established formula for the density of states without any prerequisite assumptions from SSPG theory become highly necessary for microcrystalline semiconductors. Such formula may allow for more precise determination of DOS from SSPG technique.

Acknowledgements

The author would like to thank the Higher council of Science and Technology (HCST), Jordan and the Deutsche Forschungsgemeinschaft (DFG), Bonn, Germany for their support. The author would also like to thank Dr. Rudi Brueggemann, University of Oldenburg, H. Brummack and K. Bruhne, institute fur Physikalische Elektronik, Universitat Stuttgart, for providing the experimental data and the samples. I am grateful to Professor Kh. Siddiqui for readproofing the final draft of this paper.

References

[1] R. J. Zambarno, Ph.D. Thesis, Utrecht University, The Netherlands, 2003.
[2] A. R. Moore, Semiconductors and Semimetals, 1st ed. (McGraw-Hill, New York, 1984).
[3] D. Ritter, K.Weiser, E. Zeldov, J. Appl. Phys. **62,** 4563 (1987).
[4] D. Ritter, E. Zeldov, K. Weiser, Appl. Phys. Lett. **49,** 791 (1986).
[5] D. Ritter, K. Weiser, E. Zeldov, Phys. Rev. B, **38,** 8296 (1988).
[6] C. D. Abel, G. H. Bauer, W. H. Bloss, Phil. Mag. B, **72,** 551 (1995).
[7] Y.M. Li, Phys. Rev. B, **42,** 9025 (1990).
[8] K. Hattori, H. Okamoto, Y. Hamakawa, Phys. Rev. B, **45,** 1126 (1992).
[9] R. Brueggemann, University of Oldenburg, Germany (Private Communication 2004).
[10] R. Brueggemann, R. I. Badran, Mat. Res. Soc. Symp. San Francisco-USA, Vol. **808,** A9.7.1 (2004).
[11] R. I. Badran, J. Mat. Sci.: Materials to Electronics 18, 405 (2007).
[12] R. I. Badran, N. Al_Awaad, J. Optoelectron. Adv. Mater. **8,** 1466 (2006).
[13] J. A. Schmidt, C. Longeaud, Appl. Phys. Let. **85,** 4412 (2004).
[14] J. A. Schmidt, C. Longeaud, Phys. Rev. B, **71,** 125208 (2005).
[15] R. S. Brueggemann, O. Kunz, Phys. Status Solidi B **234,** R16 (2002).
[16] R. Brueggemann, J. Mat. Sci: Materials in Electronics **14,** 629 (2003).
[17] T. Dylla, F. Finger, E. A. Schiff, Appl. Phys. Lett. **87,** 0321103 (2005).
[18] L. C. Cheng, S. Wagner, Appl. Phys. Lett. **80,** 440 (2002).
[19] J. P. Kleider, M. Gauthier, C. Longeaud, D. Roy, O. Saadane, R. Brueggemann, Thin Solid films **403-404,** 188 (2002).
[20] J .P. Kleider, C. Longeaud, M. Gauthier, M. Meaudre, R. Meaudre, R. Butte, S. Vignoli, P. Roca I Cabarrocas, Appl. Phys. Lett **75,** 3351 (1999).
[21] S. Reynolds, V. Smirnov, F. Finger, C. Main, R. Carius, J. Optoelectron. Adv. Mater. **7,** 91 (2005).

*Corresponding author: rbadran@hu.edu.jo; rbadran_i@yahoo.com